Vacuum photodiode detector array for broadband UV detection in a tokamak plasma[a)]

S. J. Zweben, C. R. Menyuk,[b)] and R. J. Taylor

Center for Plasma Physics and Fusion Engineering, University of California, Los Angeles, California 90024

(Received 20 February 1979; accepted for publication 10 April 1979)

An array of vacuum photodiode detectors has been used to monitor discharge equilibrium, stability, and cleanliness in the Macrotor tokamak. These detectors use the photoelectric effect on small tungsten plates to measure UV emission in the band $\lambda \sim 200$–1200 Å, and so are sensitive mainly to impurity line radiation in Macrotor. The response of this system to controlled impurity contamination experiments and to disruptions is described. The design, construction, and background problems associated with these detectors are discussed in detail.

INTRODUCTION

This report describes a new tokamak diagnostic which has a broadband response to UV radiation in the range $\lambda \sim 200$–1200 Å. The detectors are simply small metal plates located inside the Macrotor vacuum vessel (minor radius = 45 cm) but outside the plasma, from which a photoelectric current proportional to the incident UV flux is emitted. A two-dimensional array of these detectors has provided information about discharge equilibrium, stability, and cleanliness.

The need for spatially resolved radiation diagnostics in tokamak research has become clear. An EUV silicon diode array sensitive to $\lambda \sim 5$–20 Å was used on ST to estimate high-Z impurity contamination,[1] and collimated soft x-ray PIN diode detectors are now routinely used to study instabilities in hot ($T_e \sim 500$ eV) tokamaks.[2] More recently, silicon surface barrier detectors have been used to measure spatial radiation profiles in the hard-UV range ($h\nu \sim 100$ eV).[3,4] There also exist spatially resolved bolometric[5,6] and impurity line radiation systems,[7,8] but there has not yet been a broadband diagnostic for the important region $\lambda \sim 100$–1000 Å.

The present system was motivated by the need for a monitor of discharge equilibrium for Macrotor which (at $T_e \sim 100$ eV) does not emit significantly in the soft x-ray region. In this case vacuum photodiode (VP) detectors act qualitatively like bolometers, since most of the radiated power is expected at $h\nu \gtrsim T_e$. Thus for monitoring the edge radiation of hotter plasmas this system may be considered as complementary to the silicon detectors (which cannot respond below $\lambda \sim 50$–500 Å due to a surface dead layer). It should be noted, however, that the vacuum photodiodes respond only to the number of incident photons in the sensitive range, and so cannot be used as a quantitative bolometer for measurement of the total radiated power from the tokamak.

This detection scheme is better in some ways than PIN or silicon barrier detectors for studying tokamak plasma radiation. The advantage of the present system lies in its simplicity and low cost, and its natural sensitivity in a wavelength region which is not accessible to other systems. While the background problems discussed in Sec. II may have to be reassessed for hot-neutral-beam driven machines, the apparent immunity of the VP detectors to hard x-ray and (probably) neutron backgrounds may make these detectors attractive for use in future tokamak devices, especially in conjunction with a total radiation detection system.

The photoelectric effect itself is well documented for the region $\lambda \sim 200$–1200 Å. The advent of syncrotron sources for UV has recently stimulated study in the difficult region $50 < \lambda < 200$ Å as well,[9] but this range of low photoelectric yield is not too significant for the present investigation. There have been many detailed investigations of photoelectron emission using vacuum photodiodes, including those in which the spectrum of emitted electrons is useful for unfolding the incident UV spectrum,[10] and those aimed primarily at studying the properties of the metal itself.[11] Vacuum photodiode transfer standards have been developed at the National Bureau of Standards for use in absolute calibration of VUV spectrometers,[12] but apparently this simple device has not yet been used as a broadband monitor of tokamak radiation, although x-ray diodes have been used previously in laser fusion research.[13]

I. PRINCIPLES OF OPERATION

The photoelectric yield of tungsten has a broad peak in the range 200–1200 Å with an average yield in this range of about 0.1 electron per photon.[14] This wavelength region involves the "volume" photoeffect, and so electron emission is expected to be much less dependent on surface conditions than are detectors for higher UV wavelengths.[15,16] The choice of tungsten as our photoelectron emitter was not critical, since other metals have essentially the same yield. In the Macrotor tokamak, the UV flux is such that a typical photoelectron current is on the order of 100 μA/cm^2, and hence easily measurable with a conventional current amplifier.

A schematic drawing of our detector configuration is shown in Fig. 1. The photoemitting tungsten plate and its iron shield are mounted onto a glass port through

 0034-6748/79/080972-07$00.60

a vacuum BNC connector. The glass provides electrical and thermal insulation from the main chamber. The current emitted by the plate produces a voltage drop across the feedback resistor on the FET op-amp (LF357). The plate biasing, wire meshes, and iron shield are used to eliminate the effects of plasma particles and magnetic fields as discussed in Sec. II.

It is important to note that in Macrotor the VP detector assemblies are mounted about 10 cm outside the plasma edge (which is defined in Macrotor by the vacuum vessel wall) so as to minimize the collection of plasma particles by the detector. For higher-field plasma devices the detectors can probably be placed closer to the plasma because of the better confinement of escaping charged particles.

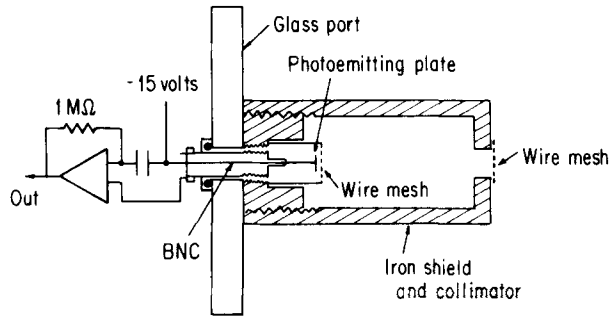

FIG. 1. Vacuum photodiode detector. Schematic drawing showing the tungsten photoemitting plate mounted inside the iron shield/collimator. The wire meshes reduce the flow of plasma to the plate. The emitted photoelectron current is measured across a 1-MΩ resistor. The plate is biased to −15 V to repel any residual plasma electrons and to insure complete emission of the photoelectrons from the plate.

II. DETECTOR DESIGN AND BACKGROUND EFFECTS

We have investigated four possible effects which might interfere with the operation of these vacuum photodiode detectors: (a) The collection of charged plasma particles by the detector plate, (b) the influence of ambient magnetic fields on the photoelectron emission process, (c) the long-term effect of surface coatings on the photoelectric yield of the plate, and (d) the background due to secondary electron emission from neutral particles. Our conclusion is that all of these effects except (d) can be made negligible in general, and that effect (d) is most likely negligible for the Macrotor tokamak.

A. Charged-particle background

A bare metal plate located near the plasma will act like a Langmuir probe and so will draw a considerable particle current depending upon its potential. In a wall plasma ($n \sim 10^{10}$ cm^{-3}, $T \sim 10$ eV) a 1-cm^2 plate will draw ~1 mA if biased to collect ion saturation current, which is a large current when compared to the ~100 μA expected from photoelectron emission (see Sec. I). The detector plate should therefore be well shielded from the plasma to avoid the collection of charged particles by the plate. This shielding is achieved in our design by placing the detectors well outside the plasma edge and by surrounding the plate by the collimator (see Fig. 1). Additional protection is then gained by biasing the plate by −15 V to repel any low-energy plasma electrons which may be inside the collimator, and by further isolating the plate from the plasma with two fine wire meshes, as shown in Fig. 1.

Several checks for the presence of a residual plasma particle background were made during normal tokamak discharges. The plate bias was swept and the voltage–current characteristic was shown to be that expected for photoemission rather than a Langmuir characteristic expected for charged-particle collection. Note that a constant signal appearing for positive plate voltages is due to a collection of photoelectrons emitted from the inside surface of the collimator. The effect of these electrons is eliminated by the −15-V bias applied to the plate during operation.

A more direct check was made by changing the orientation of the plate. With the plane of the plate oriented parallel to the axis of the collimator, the detected signal during a tokamak discharge was reduced by a factor of 10, indicating that the signal was due to a directed source from the plasma radiation and not a local isotropic plasma background.

Another indication of the absence of plasma background came from the linear increase of the UV vacuum photodiode signal with oxygen content of the discharge (see Sec. III). This increase was expected from the increased line radiation in the UV, but cannot be accounted for by any change in the wall plasma which could increase the particle background seen by the detector.

Finally, the time dependence of the vacuum photodiode signal during a tokamak discharge was compared to the output of a bare photocathode/electron multiplier located at the end of a collimated tube ~2 m away from the plasma (at which point plasma background is negligible, except for neutrals). The identity of the two signals proves that the charged particle effects are absent in the vacuum photodiodes located ~10 cm from the plasma edge. It should also be mentioned that the VP detectors placed 50 cm away from the plasma respond identically to those placed ~10 cm away at a similar location.

It is important to note, however, that for the Macrotor array the detectors located nearest the equatorial plane were <10 cm from the plasma, and that these detectors did show a background due to charged particles from the plasma. This effect appeared as a rapidly fluctuating ($f < 50$ kHz) component of the usually flat (space-averaged) VP signal. Such fluctuations in edge plasma density have been measured directly with Langmuir probes in Macrotor, and can indeed be detected at the edge of the plasma. We conclude that the detectors which showed this background effect were simply too close to the plasma edge for reliable operation.

B. Magnetic field effects

It would seem possible that the large magnetic field near the outside of a tokamak could strongly affect the photoelectric emission properties of the vacuum photodiodes. For example, a **B** parallel to the plate, combined with an E perpendicular to the plate, might result in an $\mathbf{E} \times \mathbf{B}$ drift which would cause emitted photoelectrons to strike the plate again instead of moving directly to the collimator.

The magnetic field at 10 cm outside the Macrotor plasma is $\lesssim$500 G due to the combined effects of the toroidal, vertical, and ohmic heating coils. Its direction and magnitude, therefore, vary considerably around the machine.

Since the tokamak's fields cannot be significantly changed without also changing the UV emission, we tested the VP system by superimposing a strong (500 g) dc magnetic field onto the usual fields at the detector. For a prototype detector consisting of a plate surrounded by a 1-mm-thick stainless-steel collimator, we found a 10–50% change in the amplitude of the detected signal depending upon the orientation of the applied field (the time dependence of the signal during the discharge did not change). This rather large effect prompted us to use 0.3-cm-thick iron for the collimator (see Fig. 1), which provides at least a factor of 100 magnetic shielding for the interior region (for $B < 1$ kG). A repetition of the static magnetic field test showed <5% variation in the detector signal for all orientations for this design, indicating that an applied magnetic field could no longer influence the photoelectric emission.

We should note that even without the iron in the collimator the UV signals seemed not to be affected significantly by Macrotor's normal magnetic fields. For example, the signals from a prototype UV array with only the 1-mm stainless-steel shield showed an in/out plasma UV emission symmetry even though the stray magnetic fields are strongly varying across the array. The magnetic shielding is therefore an extra protection in Macrotor, but might well be essential if these detectors are to be operated in higher-field tokamaks.

C. Surface coatings

It is well known that the photoelectric yield of metals is sensitive to surface conditions for $h\nu$ approximately equal to the work function of the metal. For the higher-energy UV photons of interest for this detector this sensitivity should diminish[15,16] since these UV photons penetrate through the surface.

We used for the detector plates small sheets of pure tungsten which had been exposed to air. The plates were cleaned in solvents to remove oil and grease, but no attempt was made to polish the surface. This procedure should result in a stable surface, if not one which is free from contaminants.

A prototype detector was operated in Macrotor over a period of 2 months, which included 1000 h of discharge cleaning and 2000 tokamak shots. The detector output was identical for identical tokamak shots observed over this time (a similar long-term stability has been observed with the whole detector array). We have, therefore, concluded that in practice any variation in these detectors due to *in situ* surface coating is negligible.

D. Neutral-particle background

Neutral hydrogen atoms emitted from the plasma can strike the plates and produce some secondary electrons which are indistinguishable from those produced by UV. The cross section for this process is $\approx$0.01 electron/neutral at 100 eV, but increases to $\approx$1 electron/neutral at 10 keV.[17] The magnitude of this background thus depends upon the fraction of power loss through neutrals compared to that lost in UV, and on the energy spectrum of the neutrals. We would expect this background to be minimal for Macrotor at $T_i \sim 50$ eV.

It is difficult to experimentally decouple the low-energy ($E < 200$ eV) neutral background from the UV signal. We have inserted an aluminum filter with a bandpass $\lambda \sim 150$–700 Å in front of the detector plate, and have observed that the signal from a tokamak discharge roughly retains its unfiltered shape versus time, but is reduced by a factor of 10 in amplitude. This behavior is consistent with that expected for UV alone, but could also be consistent with a neutral background of the same order as the UV, which coincidentally has the same shape versus time.

We have also observed that the VP signal increases linearly with the oxygen content of the discharge (see Sec. III), a behavior which is again consistent with that expected for UV and which is not consistent with any known mechanism by which the neutrals may increase in this case. In an extremely oxygen-free discharge obtained by titanium gettering, the UV signal was observed to fall about a factor of three below the usual levels as reported in this paper, confirming that the signals in the usual case were not dominated by a neutral background (which would be independent of the impurity content, other discharge parameters being equal).

We have concluded that for Macrotor the neutral background effect appears to be negligible. It is possible, however, that this may not be true for other tokamaks which may have an increased flux of neutrals relative to UV. The high-energy ($E > 200$ eV) neutral background can readily be checked by comparison with a charge-exchange analyzer. The low-energy background can probably be checked by a time-of-flight discrimination between neutrals and UV.

III. SOURCES OF UV RADIATION

A typical example of the output of a single VP detector is shown in Fig. 2. This particular detector views the central region of the plasma from the top of the machine,

and has been as a routine monitor of UV radiation for over 6 months on Macrotor.

It can be seen that the VP signal peaks at about 3–5 msec into the discharge, while H_β visible light signals peak at 1 ms. This result shows that the detector is not sensitive to visible light and also that it is not dominated in this case by UV emission from the hydrogen filling gas (which lies mostly above $\lambda \sim 900$ Å). The shape of the VP signal versus time immediately reminds us of the "burnthrough" characteristic of low-Z impurities in tokamaks, which are indeed expected to emit strongly in the UV. Also shown in the figure are O-II and O-VI lines (oxygen is the main low-Z impurity in Macrotor, and O-VI is the highest state of oxygen in these low-temperature discharges). The fact that the VP signal peaks between O-II and O-VI suggests that it may be seeing the sum of UV radiation emitted by oxygen during its burnthrough.

Another indication that the VP detector is sensitive to the impurity level comes from its response during the first few tokamak shots of a particular day's operation. During these shots some surface contamination of the walls is cleaned up, so that the high VP level of the first shots is correlated with a high impurity level (and a higher plasma resistivity). A steady-state discharge condition is usually obtained within ~5 shots.

A third indirect indication that the VP signals are due to impurity radiation comes from the behavior observed during hydrogen gas puffing. In this process the plasma density is increased, and the VP signal is seen to increase nearly linearly with the density, as would be expected since the radiated power should be proportional to n_e for a fixed temperature and impurity density.

Other possible UV emission processes include bremsstrahlung and high-Z (metal) impurity radiation. Although bremsstrahlung at $T_e \sim 100$ eV certainly produces UV, it can be estimated that the expected radiated power is much too small (10 W) to account for the observed photoelectric current detected. In fact, using an assumed $\lambda \sim 500$ Å we estimate 1–10 kW of radiated power from Macrotor in the sensitive range of this detector. This power level is inconsistent with bremsstrahlung but is consistent with the known level of impurity radiation in tokamaks.[18] The contribution from high-Z radiation cannot be discounted so easily; in fact, it has been shown that this can be the dominant loss for high-temperature discharges. It does appear, however, that the peaking of the VP signal early in time is associated with a low-Z and not a high-Z impurity.

It is of interest to determine if any impurity dominates over the others in producing the observed VP signal. Macrotor is a clean tokamak in which the low-Z impurity level can be increased significantly without destroying the discharge. We have followed the procedure outlined by Oren and Taylor[19] for varying the oxygen and carbon content of the discharges, and have correlated the increases in these impurities with the VP signals.

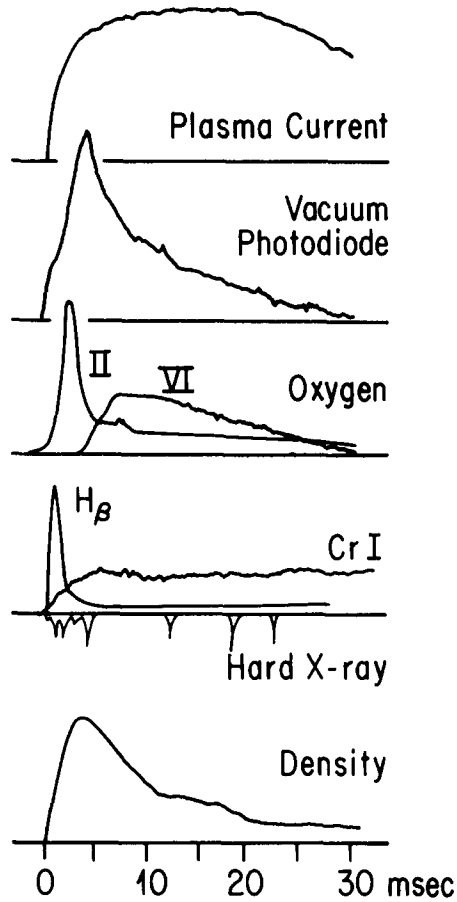

FIG. 2. Example of the vacuum photodiode signal. The VP signal peaks at 3–4 ms into this discharge, while the O-II and H_β visible light peak earlier (<1 ms), and the O-VI (1032 Å) peaks later (~8 msec). There appears to be no correlation with hard x rays or metal lines, although the contribution of metal UV lines to the steady-state VP signal cannot be discounted.

The contamination procedure involves a slow leakage of impurity gas into the chamber, so that over a large number of discharges the impurity concentration on the walls is gradually increased; during a tokamak shot the impurity content of the discharge is determined by the wall condition in the usual way.

Our results are shown in Fig. 3. It appears that the UV radiation (measured at $t \simeq 15$ ms by a detector viewing through the minor axis of the machine) increases linearly with the O-II light for a CO_2 leak, while there is no significant increase in UV radiation with increasing C-II light during a CH_4 leak. We conclude that the detector signal in these discharges is dominated by oxygen impurities rather than carbon, and that most likely the baseline (no external contamination) radiation is mainly due to oxygen. This last inference is not conclusive, however, since we have only shown that $\Delta(\mathrm{UV}) \propto \Delta$ (oxygen) by this procedure.

It is interesting to note that the oxygen impurity content can be increased by a factor of 3 (and carbon by a factor of 6) before the discharge resistivity increases significantly. This implies that for the baseline case the power balance is not dominated by radiation from these

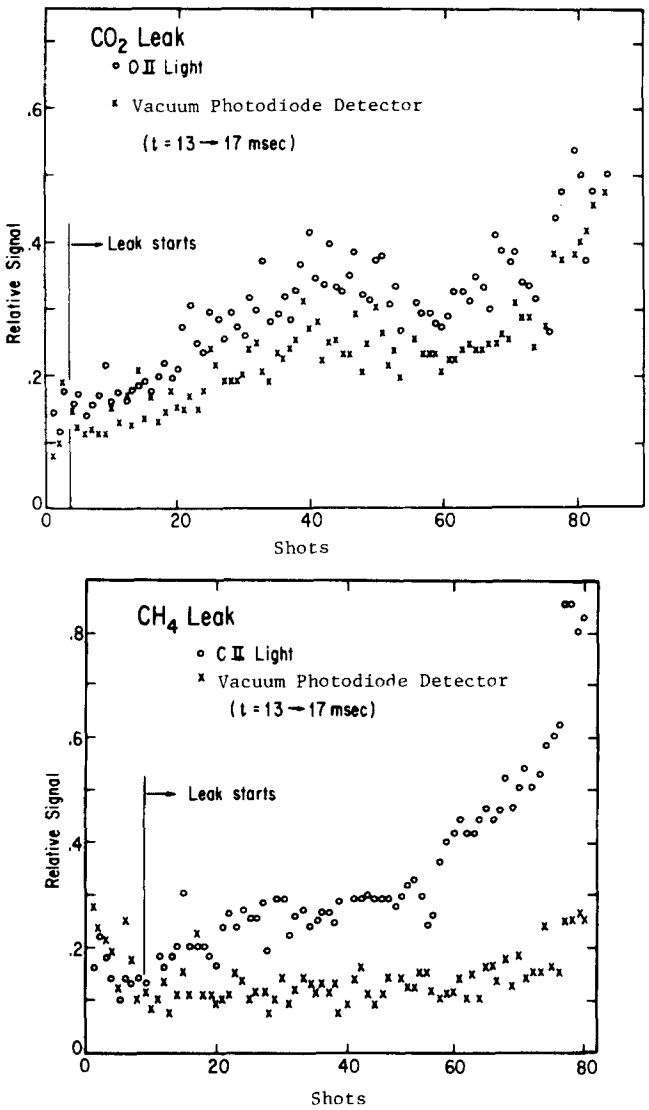

FIG. 3. Controlled impurity experiments. The correlation between the VP signal (for a detector viewing the central region of the plasma) and the oxygen and carbon content of the discharge is shown here. The VP signal increases linearly with oxygen content (as monitored by O-II), but does not increase with the carbon content (C-II). We tentatively conclude that the VP signal from the uncontaminated discharge is due mainly to oxygen radiation.

species, and also that $Z \approx 1$ for the uncontaminated discharges.

IV. VP DETECTOR ARRAY AND EQUILIBRIUM MONITORING

An array of 12 vacuum photodiode detectors has been operated on Macrotor. Six detectors viewed the plasma from the top, and six from the outside. The collimation of each of the detectors was determined by the 0.6-cm-diam hole at the end of the iron shield and by the 0.6 × 0.6-cm photoemitting plate. Thus with a standard plate–hole separation of 3.8 cm, each top detector views an area of ≈16 cm in diameter at the plasma midplane, and each side detector views a diameter of ≈10 cm at the major radius. Since all detectors are placed 15 cm apart (except S3 and S4 which are 10 cm apart), the detectors' views for each array are partially overlapping. A typical spatial profile is shown in Fig. 4.

The most straightforward application of this system is for monitoring the discharge equilibrium. *A priori*, we expect that for many systems any asymmetry in the UV profile should generally indicate an asymmetry in the positioning of the current channel. We tested this assumption by varying the plasma position by changing the vertical field while keeping the plasma current fixed. It was found that the VP array indicated that the UV profile moved in and out qualitatively as expected.

It would be useful to be able to interpret these profiles in terms of plasma temperature or density variations. In general, the total radiated power due to an impurity species is $p_r = n_e n_I f(T_e)$, where n_e is the electron density, n_I is the ion density, and $f(T)$ is a function which depends on the atomic physics. For oxygen the total radiated power falls with increasing temperature between $T_e \simeq 20$ eV and $T_e \simeq 100$ eV, which is the range of interest for the Macrotor plasma.[18] The available spectroscopic information[20] also shows that for each of O-III through O-VI most of the radiated power lies in the range $\lambda \sim 200$–1200 Å. Thus, we can tentatively say that the overall radiation from oxygen seen by the VP should also decrease with increasing temperature for $20 < T_e < 100$ eV.

Evidently, a detailed interpretation of the observed UV profiles such as Fig. 4 cannot be made at present in terms of known UV sources. For Macrotor neither $n_I(r)$ nor $T_e(r)$ is presently known, and even if they were

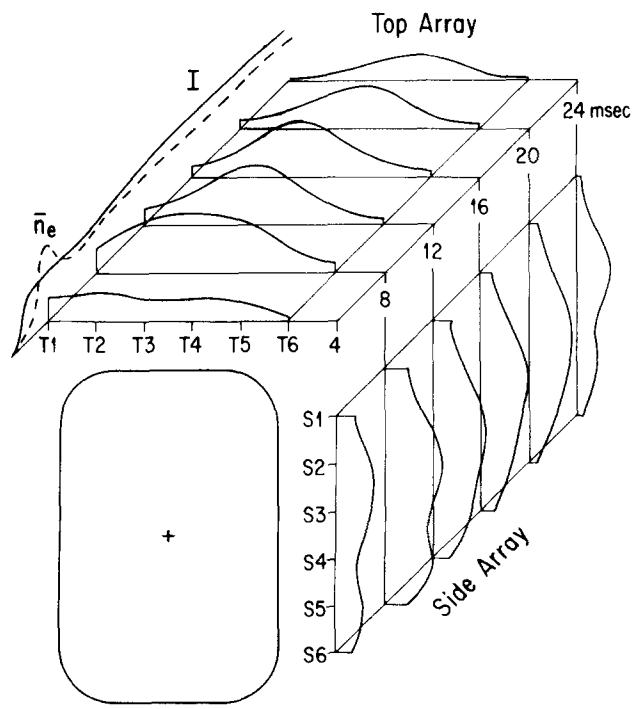

FIG. 4. UV profiles. These uninverted spatial profiles are obtained from the 6 × 6 VP array. For the side detectors S2–S4, a fluctuating component due to a charged-particle background was subtracted out (see Sec. II A). The major axis lies to the left of T1 in this figure.

known it would probably be impossible to unfold the VP into a meaningful set of UV sources (a UV spectrometer would be much more useful here.) It can be argued qualitatively that the observed UV profile reflects a combined effect of a peaked density profile (which would produce a peaked emissivity) and a peaked temperature profile (which would produce a hollow emissivity if oxygen were the dominant UV source). This argument is supported by the linear increase in the VP signals with increased n_e, and by the fact that the peak emission during a discharge comes at a time when the electron temperature is rising (see Fig. 2). We should stress, however, that the interpretation of the VP signals will vary strongly with machine parameters and contamination.

We thus conclude that the VP detectors are mainly sensitive to impurity radiation, but that a detailed use of the array for impurity studies or power balance measurements is practical only if the low-energy, low-Z radiation is dominant and the detectors are calibrated *in situ* by the method of controlled impurity contamination. The detectors are useful without such calibration for equilibrium and stability studies, and as an overall monitor of discharge impurity contamination and reproducibility.

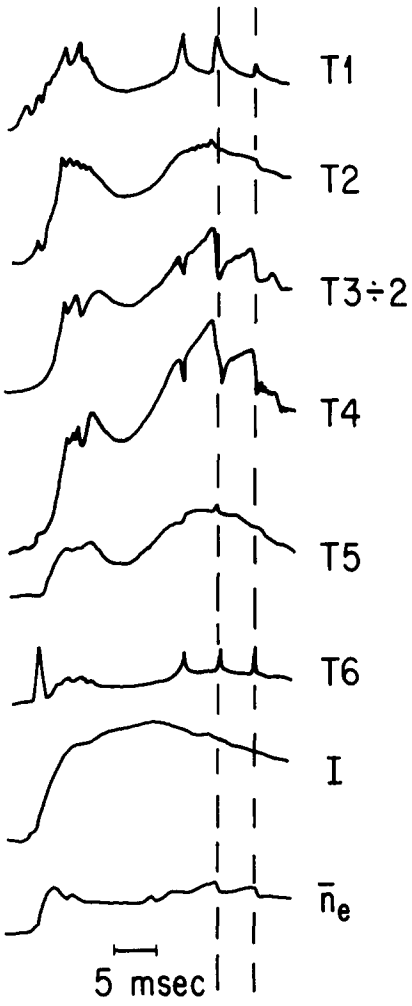

FIG. 5. Disruption during gas puffing. The response of the top detectors during gas puffing is shown here. The central detectors (T3, T4) show a drop in signal, while the outer detectors (T1, T6) show an increased signal. The side detector array responds similarly.

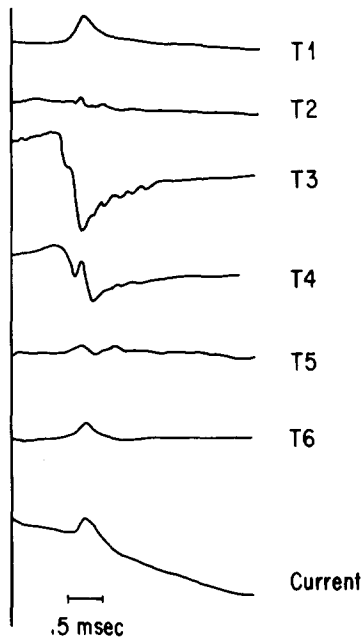

FIG. 6. Detail of disruption during gas puffing. The first disruption marked in Fig. 5 is shown here with a faster time sweep. The change in UV emission occurs simultaneously to within ~0.1 ms on all channels, and the peak perturbation occurs 0.3–0.4 ms later. The changes in UV emission in this case are probably due to the flattening of the density profile.

V. DISRUPTIONS IN THE UV

As an example of the use of this VP array for stability studies, we describe some observations of space-time-resolved UV emission during tokamak disruptions. These phenomena have been extensively studied with magnetic loops and x-ray and hard-UV ($\lambda < 200$ Å) detectors,[21] but not (to our knowledge) in the soft-UV region.

The top VP array signals during a disruptive discharge are shown in Fig. 5. Such disruptions occur in Macrotor during the dirty discharges at the beginning of a tokamak run, during gas puffing, and apparently when the discharge equilibrium is not adjusted properly. The disruptions in this figure were associated with gas puffing.

A closer view of these disruptions during gas puffing is shown in Fig. 6. Apparently, the increase in signal in the outer detectors (T1 and T6) starts at the same time (within 100 μs) as the decrease in signal at the central detectors (T3 and T4), and for both detectors the maximum change in signal occurs after ~300–400 μs. The UV emission returns to its original level with a time constant of about 1 ms. It is interesting to note that detectors T2 and T5 show very little change during this disruption, as if they were located at the node of the plasma perturbation causing the changes in the other detectors.

Possible causes of the observed perturbations include temperature, density, and impurity variations. Since the

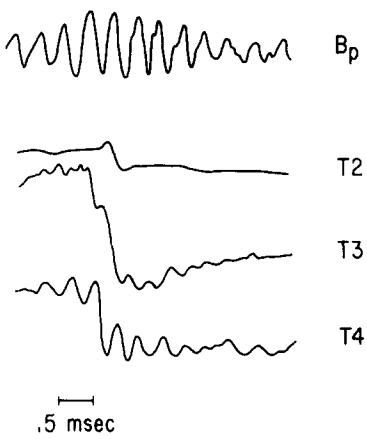

FIG. 7. Disruption with MHD activity. This expansion of the second disruption of Fig. 5 shows that some disruptions are accompanied by a growing MHD activity which can be seen on the inner VP detectors. In this case, the B_p activity began to increase about 1.5 ms before the disruption.

disruption almost certainly involves the flattening of the T_e and n_e profiles, the central decrease in UV signals correlates with a decrease in both T_e and n_e. Since we have tentatively identified the VP signals with oxygen radiation, and since oxygen UV radiation increases with decreasing temperature in the range of $20 < T_e < 100$ eV of the Macrotor plasma, we conclude that the observed variations in UV signals during this disruption are due primarily to density rather than to temperature variations. Indeed, the measured line average density through the center of this discharge does decrease significantly during these disruptions (see Fig. 5).

The second disruption in the shot of Fig. 5 is shown in Fig. 7. In this case it is clear that a growing MHD disturbance is involved, especially in the UV response of the inner detectors. Apparently, these disruptions can occur with or without MHD precursors.[3]

In Fig. 8 we show a rare "major" disruption that resulted in a dramatic drop in current which may be attributed to a strong decrease in temperature. The dramatic increase in the signal from a central VP detector is most likely due to increased impurity radiation from oxygen at this lower temperature.

Obviously, a complete description of the disruption has not been obtained with this system. Nevertheless, it is clear that these detectors can be used to monitor

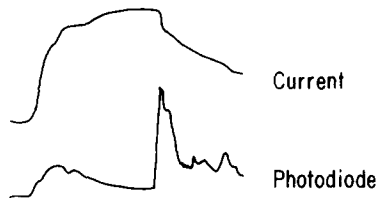

FIG. 8. Major distribution. In this example a "major" disruption resulted in the loss of a significant fraction of the plasma current. The associated plasma cooling most likely caused the oxygen radiation to increase dramatically, as seen here in a central VP detector.

stability phenomena in the UV in a manner similar to the x-ray or hard-UV systems.

[a] Research supported by USDOE Contract EY-76-C-03-0010 PA 26.
[b] Supported, in part, by the Fannie and John Hertz Foundation.

[1] N. Bretz *et al.*, in *Proc. 5th Int'l. Conf. Plasma Physics and Controlled Nuclear Fusion Research*, Tokyo, 1974, Vol. I, p. 55.
[2] S. Von Goeler, W. Stodiek, and N. Sautoff, Phys. Rev. Lett. **23**, 1201 (1974).
[3] N. R. Sautoff, S. Von Goeler, and W. Stodiek, Nucl. Fusion **18**, 1445 (1978).
[4] F. H. Seguin *et al.*, in *IEEE Int'l. Conf. on Plasma Science*, Monterey, 1978.
[5] C. E. Bush and J. F. Lyon, Oak Ridge Nat'l. Lab. Report No. ORNL-TM-6148.
[6] Equipe TFR, *Proc. 6th Int'l. Conf. Plasma Physics and Controlled Nuclear Fusion Research*, Berchtesgaden, 1976, Vol. I, p. 35.
[7] S. Suckewer, E. Hinov, and J. Schivell, Princeton Plasma Physics Lab. Report No. PPPL-1430, 1978; J. L. Cecci, PPPL Report No. MATT-1256, 1977.
[8] TFR Group Phys. Rev. Lett. **36**, 1306 (1976).
[9] R. H. Day, *et al.*, in *Second Topical Conf. on High Temp. Plasma Diagnostics*, Santa Fe, 1978 (Report LA-7160-C, LASL).
[10] L. Heroux and H. E. Hinteregger, Appl. Opt. **6**, 701 (1962).
[11] J. Romand and B. Vodar, *Vacuum Ultraviolet Radiation Physics* (Pergamon, New York, 1974).
[12] L. R. Canfield, R. G. Johnston, and R. P. Madden, Appl. Opt. **12**, 1611 (1973).
[13] V. W. Slivinski and H. N. Kornblum, Rev. Sci. Instrum. **49**, 1204 (1978).
[14] J. D. Samson, *Techniques of Vacuum Ultraviolet Spectroscopy* (Wiley, New York, 1967).
[15] W. C. Walker, N. Wainfain, and G. L. Weissler, J. Appl. Phys. **26**, 1366 (1955).
[16] A. N. Zaidel and E. Schreider, *Vacuum Ultraviolet Spectroscopy* (Ann-Arbor Humphrey Science, Ann-Arbor, MI, 1970).
[17] J. A. Ray and C. F. Barnett, J. Appl. Phys. **42**, 3260 (1971); C. F. Barnett *et al.*, Oak Ridge Nat'l. Lab. Report No. ORNL-5207, 1977 (Fig. D.3.12).
[18] C. Breton, *et al.*, Nucl. Fusion **16**, 891 (1976); see also R. V. Jenson *et al.*, Nucl. Fusion **17**, 1187 (1977).
[19] L. Oren and R. J. Taylor, Nucl. Fusion **17**, 1143 (1977).
[20] A. R. Striganov and N. S. Sventitskii, *Tables of Spectral Lines of Neutral and Ionized Atoms* (Plenum, New York, 1968).
[21] Equipe TFR, Nucl. Fusion **17**, 1283 (1977).